Kovove Mater. 55 2017 413–420
DOI: 10.4149/km_2017_6_413

Analysis of sheet surface roughness change under contact with flat and spherical indenters

T. Trzepieciński[1]*, Ł. Bąk[1], F. Stachowicz[1], S. Bosiakov[2], S. Rogosin[3]

[1] *Department of Materials Forming and Processing, Rzeszow University of Technology, Al. Powstańców Warszawy 8, 35-959 Rzeszów, Poland*
[2] *Department of Theoretical and Applied Mechanics, Belarusian State University, Niezavisimosti Avenue 4, 220030 Minsk, Belarus*
[3] *Department of Economics, Belarusian State University, Niezavisimosti Avenue 4, 220030 Minsk, Belarus*

Received 21 August 2016, received in revised form 13 september 2016, accepted 12 January 2017

Abstract

In this paper, the effect of strain hardening on the elastic-plastic contact of steel sheets is considered using experiments. The effect of normal load and the effect of prestrain of the sheets on the change of surface roughness parameter values and real area of contact are analysed. Continuous indentation tests were performed on 2 mm thick DC04 steel sheets. The mechanical properties of the sheet metal were determined using uniaxial tensile tests along three directions concerning the rolling direction. Two cylindrical and spherical indenters were used in the investigations. It can be concluded that the real area of contact between a tool and a workpiece depends on the degree of sample prestrain, normal load and different flattening and roughening mechanisms of the deforming asperities. The effect of normal force on real contact area depends on the load value. The penetration depth value increases proportionally to the normal load.

K e y w o r d s: elastic-plastic contact, contact mechanics, flattening, indentation test, surface roughness

1. Introduction

The rough surface of the sheets can be described as the collection of hill and valley or called the "asperity" [1]. Plastic deformation produces qualitative changes in the distribution of local pressures in the contact and the size of connected contact regions [2]. Real contacting surfaces are rough, leading to the concentration of contact in a cluster of microscopic actual contact areas [3]. In other words, asperity against asperity is the real contact interaction in the engineering surface [1]. In the literature, there are some studies on the simplification of the interactions between the asperity contacts. Hertz [4] proposed the theory of a static contact model in elastic condition, where the asperity was modelled as spherical and cylindrical geometries. Johnson [5] found that friction could increase the total load required to produce a contact of given size by up to 5 % compared to Hertz. Chang et al. [6] generated a static contact model in the elastic-plastic condition analytically, whereby asperity was modelled in spherical geometry. Chatterje and Saho [7] studied the effect of strain hardening on the elastic-plastic contact of a deformable sphere against a rigid flat under full-stick contact conditions. The fractal models of surface asperities ignored the interactions between adjacent asperities and considered small deformation [8, 9]. Pei et al. [2] extended the findings of elastic contact to investigate the influence of elastic properties of the material in the elastoplastic phase by considering a wide range of self-affine surface topographies. They concluded that plastic deformation acts as an equaliser that reduces the effect of material and surface properties. They also found that the total plastic dissipation during deformation is roughly independent of yield stress for typical yield stress values. Brizmer et al. [10] developed a model for elastic-plastic contact between a deformable sphere and a rigid flat under combined

*Corresponding author: tel.: +4817 8651714; e-mail address: tomtrz@prz.edu.pl

normal and tangential loading with full-stick contact conditions. The indentation test can also be used to observe the influence of the applied test loads and microstructure on the measured hardness [11] or to the structural and mechanical characterisation of alloys [12].

Greenwood and Williamson [13] developed the method of calculation of contact characteristics of rough surfaces. Pei et al. [2] investigated theoretically the behaviour of an elastic-plastic contact between a deformable sphere and a rigid flat with full-stick contact conditions. They found that at low normal dimensionless loads the static friction coefficient decreases sharply with increasing normal load. Shankar and Mayuram [14] show that the transition behaviour of the materials from the elastic-plastic to the fully plastic case is influenced by the yield strength. The experimental results of the work done by Ovcharenko et al. [15] indicate an irreversible process leading to an increase in the contact area with an increasing number of loading cycles but with a clear tendency to shake down.

Real surfaces are rough on the microscale and consist of asperities of different shapes and sizes [15]. An accurate knowledge of the real contact area is important for studies involving many frictional and contact mechanic issues. Understanding the friction phenomenon and the surface qualities requires sufficient knowledge of the tribological behaviour at the interface between a tool and a workpiece. The friction force depends on a number of parameters, such as the sliding speed, surface roughness, normal load and lubrication conditions [16, 17]. The realistic friction models must also treat the influence of roughness asperities and surface topography on the lubricant flow and the asperity contact [17, 18]. The adhesive and frictional forces between two solids arise from regions where their atoms are close enough to interact. The area and geometry of contact area influence the elastic and plastic deformation that extends well below the surface [2]. Ploughing effects between asperities and adhesion effects between boundary layers are the main factors causing friction in the boundary lubrication regime [19]. In the case of metallic materials, some theories considering the elastic-plastic deformation of asperities have been established to explain the contact mechanism by predicting the real area of contact [5, 20, 21]. The real area of contact plays an important role in friction mechanism and relies on the roughness of both the tool and the sheet surface [22].

An adequate description of contact mechanisms in sheet metal formation requires experimental analysis of surface roughness variation during the deformation of asperities. In this paper, the analysis of roughness asperities flattening during the indentation test is analysed. Two cylindrical and spherical indenters were used in the investigations. The effect of normal load and strain hardening phenomenon on the change of surface roughness parameters values are analysed. The effect of a strain of prestrained sheet specimens cut along the rolling direction and transverse to the rolling direction is also considered.

Fig. 1. The view of the work-stand (a): 1 – indenter, 2 – specimen, 3 – self-aligning anvil.

2. Material and method

Continuous indentation tests were performed on 2 mm thick DC04 steel sheets. The samples for indentation tests were cut in two directions: along the rolling direction and transverse to the rolling direction. The flat samples of 20 mm width and 200 mm length were straightened using the uniaxial tensile test to different strain values ε_1: 5, 10, 15, 20, 25, and 30 %.

The indentation tests were performed using a modified Zwick Roell Z030 operating in the compression mode. The applied load versus the crosshead displacement or depth of the indentation was continuously recorded throughout the tests. Two indenters with flat and spherical ends were used. In our analyses, the spherical indenter made of bearing steel had a diameter of 6 mm. The cylindrical indenter made of alloy steel had a diameter of 6 mm. A maximum load F_N of 60, 80, 100, 125, 150, 200, 250, and 300 N was applied for each sample tested using the spherical indenter. In the case of cylindrical indenter with the flat contact area, we used the loads F_N: 1000, 1500, 2000, 2500, and 3000 N. The working surface of the indenter was electromachined to establish the uniform isotropic surface roughness average of $S_a = 1.745\,\mu m$. The indentation experiments using the cylindrical indenter were carried out using a special device (Fig. 1) mounted on a typical tensile machine Zwick Roell Z030. The self-aligning anvil (Fig. 2) assures the perpendicular contact of the indenter surface and deformed surface.

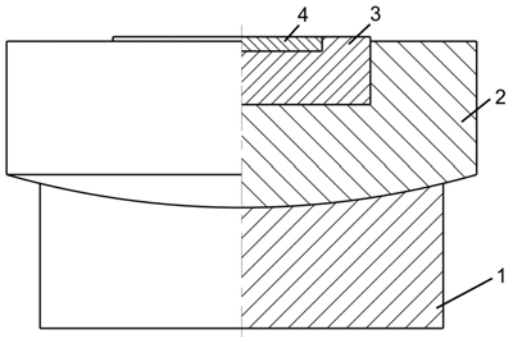

Fig. 2. Schematic of self-aligning anvil: 1 – guiding stand, 2 – self-aligning table, 3 – supporting plate, 4 – specimen.

A DC04 steel sheet was the material used in the experiments. The mechanical properties of the sheet metal were determined using uniaxial tensile tests along three directions concerning the rolling direction. The mechanical properties determined in this test (as given in Table 1) are yield stress $R_{p0.2}$, ultimate strength R_m, Lankford's coefficient r, strain hardening coefficient C, and strain hardening exponent n. The samples for the tensile tests were cut in three directions: along the rolling direction (0°), transverse to the rolling direction (90°), and at an angle of 45° concerning the rolling direction. The plastic anisotropy factor, r, was determined by the relationship between the width strain and thickness strain in the whole range of specimen elongation using the least square method. Strain hardening exponent, n, is correlated to changes in the microstructure of a material and in some ways represents processes occurring during deformation. It is used to characterise the formability of sheet material. The n-value is strain dependent and results from changes in the crystallographic texture [23]. The r-values of the sheets clearly show that the used steel sheets exhibited anisotropic properties. The values of tensile parameters (X) determined in three directions were averaged according to the formula:

$$X_{mean} = \frac{X_0 + 2X_{45} + X_{90}}{4}, \quad (1)$$

where the superscripts refer to the specimen orientation.

The measurement of surface roughness parameters was carried out using the Alicona InfiniteFocus instrument. The main standard 3D parameters determined by this measurement are: the surface roughness average S_a, maximum valley depth of selected area S_v, reduced valley height (mean depth of the valleys below the core material) S_{vk}, maximum peak height of selected area S_p, ten point height of selected area S_{z10}, core roughness depth S_k, peak material component (the fraction of the surface which consists of peaks above the core material) S_{mr1}, peak material compo-

Table 1. Mechanical properties of DC04 steel sheet

Sample orientation	$R_{p0.2}$ (MPa)	R_m (MPa)	r	C (MPa)	n
0°	182.1	322.5	1.751	549.3	0.214
45°	196	336.2	1.124	564.9	0.205
90°	190	320.9	1.846	541.6	0.209
mean value	191.03	328.95	1.461	555.18	0.208

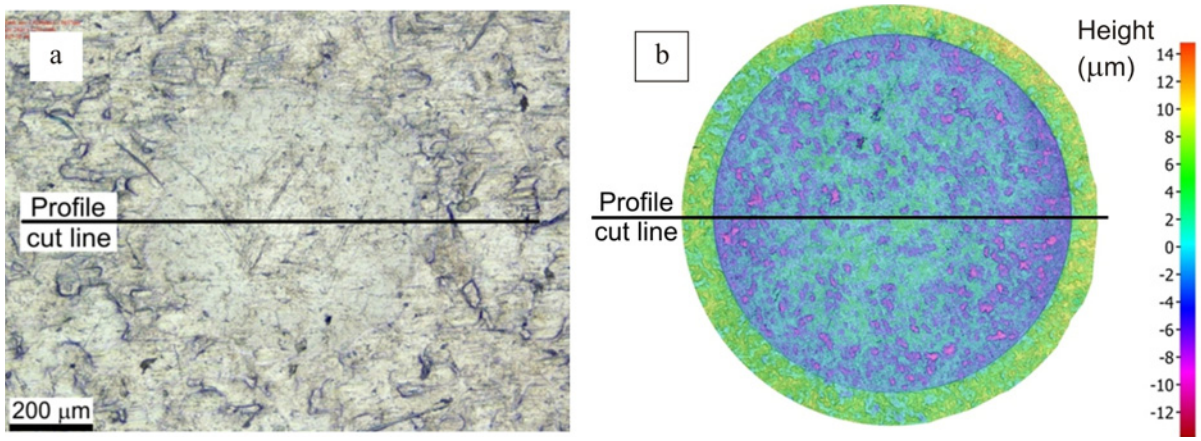

Fig. 3. Optical micrograph of indentation for spherical (a) and cylindrical (b) indenter.

nent (the fraction of the surface which will carry the load) S_{mr2}, peak material volume of the topographic surface V_{mp}, core material volume of the topographic surface V_{mc}, and core void volume of the surface V_{vc}.

The value of surface roughness parameters was determined along the profile cut line shown in Figs. 3a,b for spherical and cylindrical indenters, respectively. Furthermore, in the case of indentation tests performed using a spherical indenter the roughness parameters were determined along the rolling direction of the sheet and transverse to the rolling direction. The results of the measurements are the variations of the profile height. Typical profiles are presented in Figs. 4a,b for spherical and cylindrical indenters, respectively.

3. Results and discussion

3.1. Roughness average

The values of the *Ra* parameter measured along the rolling direction (orientation 0°) and transverse to the rolling direction (orientation 90°) of the sheet metal increased with the tensile strain level (Fig. 5). This dependence is nearly linear ($R^2 > 0.91$), which supports the work of Stachowicz [24]. In the case of *Ra* parameter measured along the rolling direction in the range of strain between 0 and 20 %, a fast increasing of its value is observed. After exceeding the value of strain of 20 % the value of the *Ra* parameter measured at 0° according to the rolling direction increased a little. Simultaneously, the value of the *Ra* parameter measured transverse to the rolling direction of the sheet constantly increases throughout the whole range of sample prestrain. Strain hardening of surface roughness limits the change of surface roughness average *Ra* of the sheet as a result of uniaxial strain on the sample. The increase in surface roughness of the sheet is the result of reorientation and fragmentation of the individual grains, mainly in the subsurface. Creation of dislocation boundaries, as well as the subdivision of the initial grains into smaller elements, are two sources of hardening [25]. Grain orientation fragmentation refers to the tendency for the lattice of different regions of grain to rotate under the deformation toward a small number of distinctly different orientations [26]. The strain hardening of the sheet metal due to plastic prestrain limits the surface topography change during indentation test [17, 23].

3.2. Indentation depth

The indentation depth h is measured between the average line of the profile curve and the average line of the indentation profile (Fig. 4a). The linear dependence between the normal load and impression depth

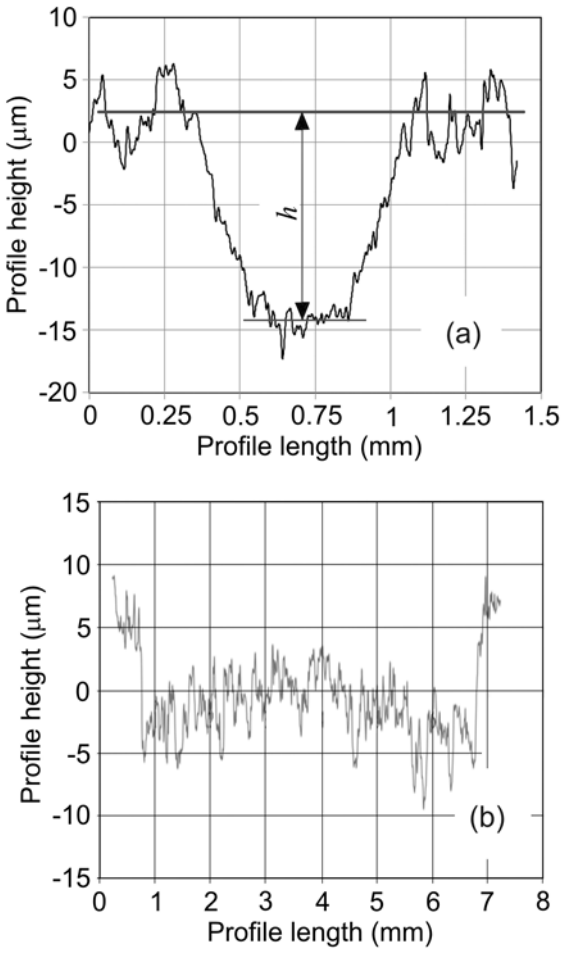

Fig. 4. Variation of the profile height along the profile cut line for spherical (a) and cylindrical (b) indenter; normal load 300 N.

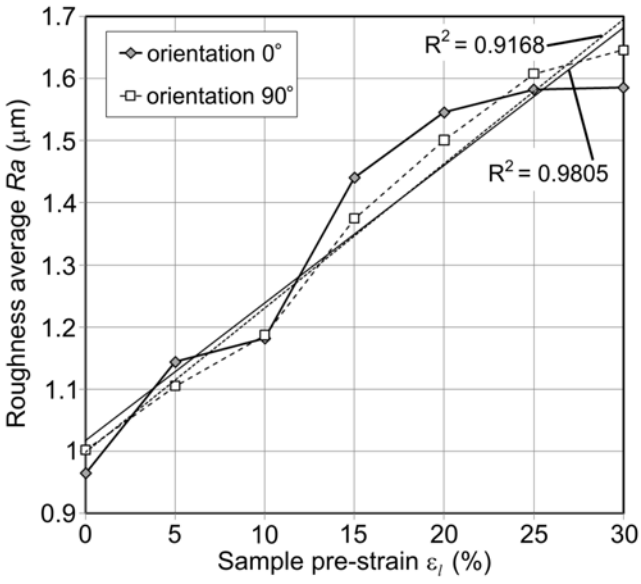

Fig. 5. Effect of sample prestrain on the change of the *Ra* parameter value in the case of samples tested using spherical indenter.

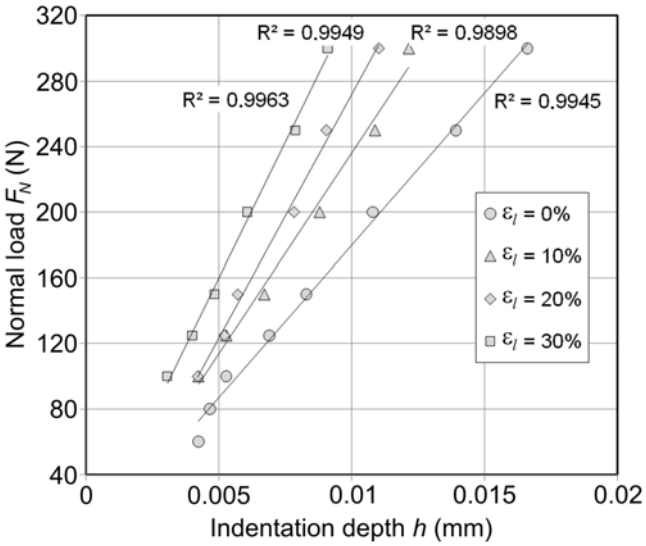

Fig. 6. Effect of indentation depth on normal load value for samples cut along the rolling direction found using spherical indenter.

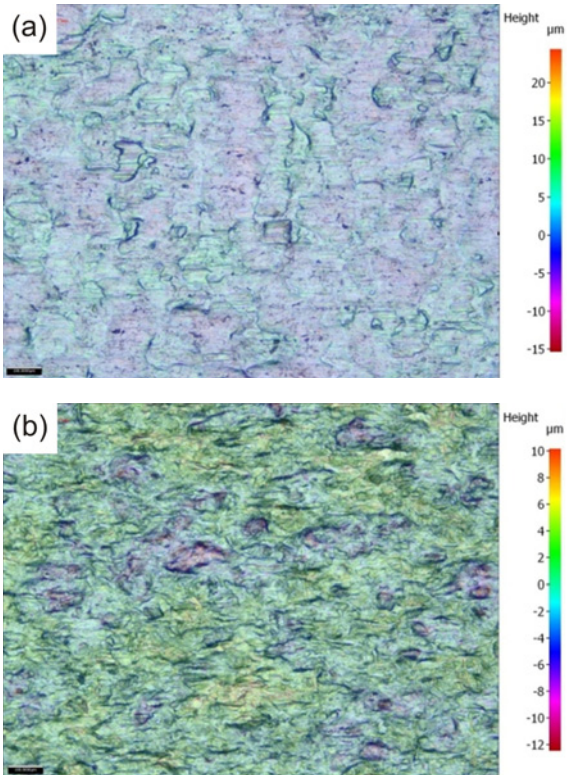

Fig. 7. Views of the surface of the steel sheet tested using a spherical indenter: original surface (a) and the surface of the sheet prestrained to 30 % (b).

is observed (Fig. 6). Furthermore, it is evident that increasing the indentation depth load allows for an increase in the normal load. It was found that the

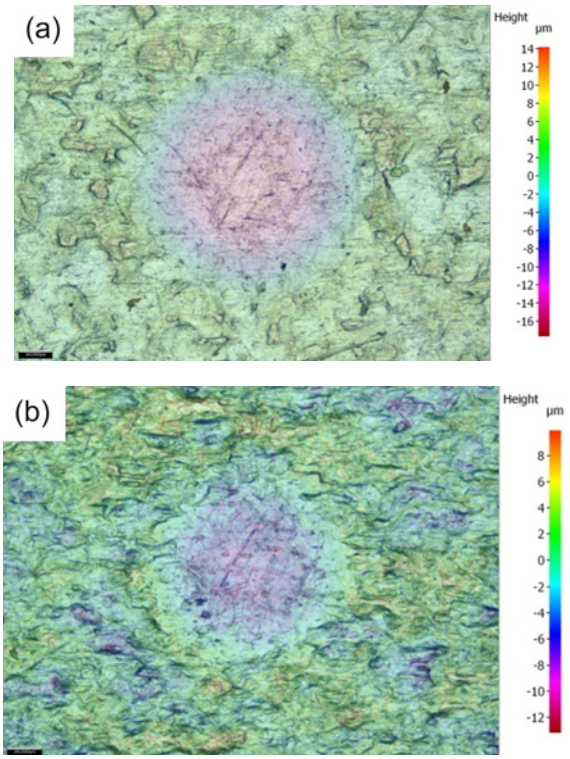

Fig. 8. Views of the indentation of the original surface (a) and the surface of the sheet prestrained to 30 % (b) and tested using spherical indenter, corresponding to normal load 300 N.

value of normal load for a specific penetration depth value increases non-proportionally with the increase of sample strain. The relation between normal load and penetration depth is nearly linear ($R^2 > 0.98$). For the samples prestrained by the highest value of strain (30 %) the fastest increase of normal load with increasing penetration depth is observed. A decrease in prestrain value leads to a smaller increase of normal load with the penetration depth. This finding is a result of an increase of deformation resistance due to the strain-hardening phenomenon and furthermore, despite the linear relationship between the normal load and penetration depth, the real contact area between the ball and sheet increases nonlinearly with the penetration depth.

The surface topography of prestrained sheet exhibits directional topography (Fig. 7b) compared to the original surface (Fig. 7a). The views of indentation before (Fig. 8a) and after prestraining (Fig. 8b) allow us to conclude that the real contact area depends on the degree of sheet deformation. It should be pointed out that the prestrain of the sheet influences a decrease of the profile height of the sheet surface. The total height of the original profile is about 40 µm (Fig. 7a), while after prestrain to 30 % the total height of the sheet surface is about 22 µm (Fig. 8a). In the

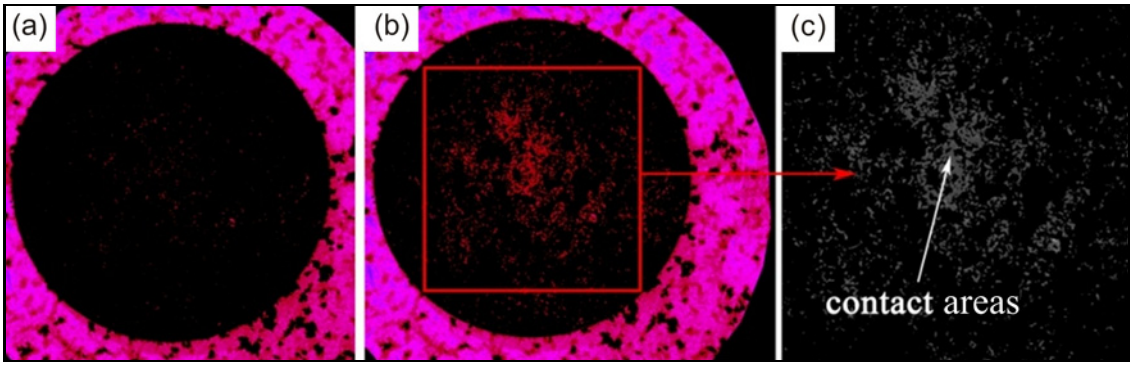

Fig. 9. The view of indentation area (a) and views of contact areas before (b) and after (c) image processing.

case of non-prestrained sheet, the area of contact of indenter and sheet is uniform (Fig. 8b), and the value of indentation depth is smaller than the value of the maximum height of the roughness profile. This fact leads to the conclusion that only the asperities of the surface were deformed. Sanchez and Hartfield-Wunsch [27] found that roughening of the surface, observed during deformation of the bulk material without applying a normal load, tends to decrease the real area of contact. Increasing the normal load to 300 N during the indentation test of non-prestrained samples causes plastic deformation to occur in the subsurface, some distance below the roughness profile. However, the strain-hardening phenomenon, in the case of prestrained samples, causes that indentation area to be smaller (Fig. 7b) than in the case of indentation of non-prestrained samples under the same load condition (Fig. 7a).

3.3. Area of contact

The evaluation of normal pressure in the case of small normal loads is a problematic issue because only the asperities of the roughness undergo a deformation. To evaluate normal pressure, there is a necessity to evaluate the real contact area, which is a dominant factor influencing the frictional phenomenon of the tested deep-drawing quality sheet. Thus, the use of tools with low surface roughness values to reduce the frictional resistance is unfounded because the increased real contact area increases the interatomic interactions of surfaces. This phenomenon increases the frictional resistance. The main asperity flattening mechanisms during sheet metal forming, which tend to increase the real area of contact, are flattening due to normal loading and flattening due to combined normal loading and deformation of the underlying bulk material [28].

The contact area was estimated via two-step analysis using IF-Measure Suite and Matlab software. In the first step, the colour range of depth image was adjusted to demonstrate only the peaks of the material located in the indented area (Fig. 9a). It was assumed

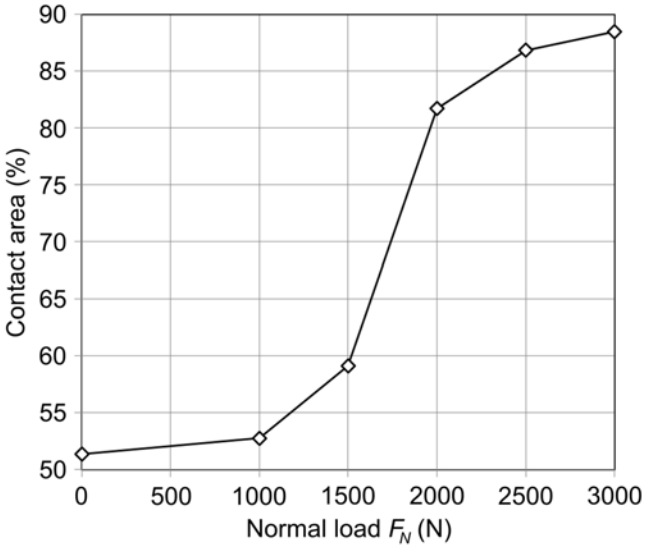

Fig. 10. Effect of normal load on the contact area evaluated during the test using cylindrical indenter.

that the contact surface is the section area 1 μm below the asperities peaks. This section was obtained by reducing a lower range of the depth image with the value of 1 μm (Fig. 9b). The second step was the processing of the selected area by short script, whereby the RBG image was converted to black and white (Fig. 9c). The real contact area is defined as the ratio of a number of black and non-black pixels.

The changes in the contact interface under increasing normal load are presented in Fig. 10 to quantify the relationship between the normal force and the contact area. In the range of normal force values up to 1500 N, a slow increase of contact area is observed. At low normal force values the load is carried out by asperities, so the contact area is not subjected to significant changes. After reaching the specific normal force value, the load is carried out by asperities and also plastic deformation occurring in the subsurface, some distance below the roughness profile. Thus, the intensity of increase of the contact area value gets smaller with an increase in the normal load. Hol et al. [28]

Table 2. Effect of normal load on variation of values of selected surface roughness parameters

Normal force (N)	Roughness parameter								
	S_k (μm)	S_v (μm)	S_p (μm)	S_{vk} (μm)	S_{mr1} (%)	S_{mr2} (%)	V_{mp} ($m^3\,m^{-2}$) ($\times 10^{-8}$)	V_{mc} ($m^3\,m^{-2}$) ($\times 10^{-8}$)	V_{vc} ($m^3\,m^{-2}$) ($\times 10^{-8}$)
0	5.3069	11.1422	9.1823	3.8261	4.57	78.24	6.31	258.88	244.66
1000	4.5062	9.7645	7.0431	4.2074	4.26	75.56	5.37	248.1	218.3
1500	3.9659	9.9613	7.4426	4.3711	4.75	73.64	5.18	238.07	202.49
2000	3.4263	10.2132	6.9037	4.4249	5.39	72.66	5.01	223.01	183.71
2500	2.9166	9.9984	8.3469	4.4631	6.2	72.2	4.76	204.66	163.41
3000	2.5916	10.2342	7.0463	4.4697	6.51	73.32	4.44	178.11	143.28

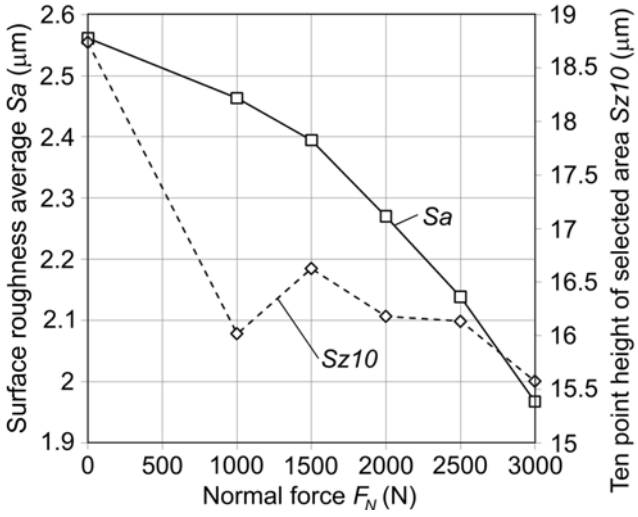

Fig. 11. Effect of normal load on the variation of surface roughness parameters S_a and S_{z10} during the test using cylindrical indenter.

found that roughening of the surface, observed during deformation of the bulk material without applying a normal load, tends to decrease the real area of contact.

3.4. Sheet surface roughness change

The surface roughness average S_a parameter value decreases monotonically with an increase of the normal load (Fig. 11). The value of the height of the profile represented by the ten-point height of selected area S_{z10} is quite stable for the whole range of used normal loads. It confirms that the load is carried out by roughness asperities and subsurface of the roughness profile. An increase in the contact pressure increases the real area of the contact, and the number of places of contact is reduced because the single contact areas are connected with each other. The phenomenon of connecting local frictional joints and then their destruction during contact is accidental. Analysing the data in Table 2, we can conclude that increasing the normal load causes:

– decreasing the value of the core roughness depth S_k,

– increasing the value of reduced valley height S_{vk},

– decreasing the value of peak material volume of the topographic surface V_{mp},

– decreasing of the core material volume of the topographic surface V_{mc},

– decreasing the value of core void volume of the surface V_{vc}.

The shape of the contact surface influences the type of contact and the state of stress in the contact areas, both in the surface layer and in the whole volume of the deformed metal. The achievement of a full, so-called nominal surface area of contact of the tool with the deformable material is limited by the strain-hardening phenomenon. The deformed asperities of the surface can transmit the load deeper into the material. The value of the real contact area and the stereomechanical structure of the surface depending on the surface roughness are closely related to the values of the frictional resistance of materials. Macrogeometry of the contact surface influences the type and nature of contact phenomena, especially in the initial stage of plastic deformation. This leads to the formation of local stress concentrations that cause the formation of microwelds and adhesions. The state of surface asperities after the deformation process is the result of many factors and is generally difficult to predict. However, the nature of the contact phenomena also influences the change of surface topography of the tool. The hardness and strength of the tool are greater than that of the deformed material, while created after tool machining the surface asperities may be the cause of creating local stress concentrations, which create the conditions for the development of micro-cracks.

4. Summary and conclusions

Roughening of asperities, observed during sheet metal forming, tends to decrease the real area of con-

tact, resulting in a lower coefficient of friction. There are two dominant mechanisms of flattening: flattening due to micro-sliding and flattening due to normal load, which was the topic analysed in our article.

The real area of the contact between a tool and a workpiece depends on the degree of sample prestrain, normal load and different flattening and roughening mechanisms of the deforming asperities. In the case of both indenter shapes, the effect of normal force on the real contact area depends on the load value. In the range of normal force values up to 1500 N slow increasing of the contact area of the cylindrical indenter and sheet is observed. After reaching the specific normal force value, the load is carried out by asperities and also plastic deformation occurring in the subsurface, some distance below the roughness profile.

The values of the *Ra* parameter measured along the rolling direction and transverse to the rolling direction of the sheet metal increased with the tensile strain level. These relations are nearly linear. The penetration depth value of the spherical indenter increases proportionally to the normal load. It was also found that the value of the normal load for a specific penetration depth value increases non-proportionally with the increase of sample strain. We can conclude that the strain-hardening phenomenon has a significant influence on the indentation value and changes the surface roughness.

Acknowledgements

The research leading to these results has received funding from the People Programme (Marie Curie International Research Staff Exchange) of the European Union's FP7/2007-2013/under REA grant agreement No. PIRSES-GA-2013-610547.

References

[1] Kartini, Saputra, E., Ismail, R., Jamari, J., Bayuseno, A. P.: MATEC Web of Conferences, *58*, 2016, p. 04007. doi:10.1051/matecconf/20165804007
[2] Pei, L., Hyun, S., Mollinari, J. F., Robbins, M. O.: J. Mech. Phys. Solids, *53*, 2005, p. 2385. doi:10.1016/j.jmps.2005.06.008
[3] Barber, J. R., Ciavarella, M.: Int. J. Solids Struct., *37*, 2000, p. 29. doi:10.1016/S0020-7683(99)00075-X
[4] Hertz, H.: Journal für die Reine und Angewandte Mathematik, *92*, 1882, p. 156. doi:10.1515/crll.1882.92.156
[5] Johnson, K. L.: Contact Mechanics. Cambridge, Cambridge University Press 1985.
[6] Chang, W. R., Etsion, I., Bogy, D. B.: ASME J. Tribol., *109*, 1987, p. 257. doi:10.1115/1.3261348
[7] Chatterjee, B., Sahoo, P.: Adv. Tribol., *2012*, 2012, p. 1. doi:10.1155/2012/472794
[8] Majumdar, A., Tien, C. L.: Wear, *136*, 1990, p. 313. doi:10.1016/0043-1648(90)90154-3
[9] Majumdar, A., Bhushan, B.: ASME J. Tribol., *112*, 1990, p. 205. doi:10.1115/1.2920243
[10] Brizmer, V., Kligerman, Y., Etsion, I.: Tribol. Lett., *25*, 2007, p. 61. doi:10.1007/s11249-006-9156-y
[11] Majić Renjo, M., Rede, V., Ćurković, L.: Kovove Mater., *52*, 2014, p. 299. doi:10.4149/km_2014_5_299
[12] Cinca, I., Novocin, A., Raducanu, D., Gloriant, T., Gordin, D. M., Dan, I., Caprarescu, A., Cojocaru, V. D.: Kovove Mater., *53*, 2015, p. 17. doi:10.4149/km_2015_1_17
[13] Greenwood, J. A., Williamson, J. B. P.: P. Roy. Soc. Lond. Ser-A, *295*, 1966, p. 300. doi:10.1098/rspa.1966.0242
[14] Shankar, S., Mayuram, M. M.: Int. J. Solids Struct., *45*, 2008, p. 3009. doi:10.1016/j.ijsolstr.2008.01.017
[15] Ovcharenko, A., Halperin, G., Verberne, G., Etsion, I.: Tribol. Lett., *25*, 2007, p. 153. doi:10.1007/s11249-006-9164-y
[16] Trzepieciński, T.: Arch. Civ. Mech. Eng., *10*, 2010, p. 95. doi:10.1016/S1644-9665(12)60035-1
[17] Lemu, H. G., Trzepieciński, T.: Stroj. Vestn.-J. Mech. E., *59*, 2013, p. 41. doi:10.5545/sv-jme.2012.383
[18] Trzepieciński, T., Lemu, H. G.: Stroj. Vestn.-J. Mech. E., *60*, 2014, p. 51. doi:10.5545/sv-jme.2013.1310
[19] Hol, J., Cid Alvaro, M. V., de Rooij, M. B., Meinders, T.: Wear, *286–287*, 2012, p. 66. doi:10.1016/j.wear.2011.04.004
[20] Maegawa, S., Itoigawa, F., Nakamura, T.: Tribol. Int., *92*, 2015, p. 335. doi:10.1016/j.triboint.2015.07.014
[21] Adams, G. G., Nosonovsky, M.: Tribol. Int., *33*, 2000, p. 431. doi:10.1016/S0301-679X(00)00063-3
[22] Hol, J., Meinders, V. T., Geijselaers, H. J. M., van den Boogaard, A. H.: Tribol. Int., *85*, 2015, p. 10. doi:10.1016/j.triboint.2014.12.017
[23] Stachowicz, F., Spišak, E.: The Methods of Assessment of Ability of Thin Sheets for Cold Metal Forming. Rzeszów, Oficyna Wydawnicza Politechniki Rzeszowskiej 1998 (in Polish).
[24] Stachowicz, F.: Acta Mech., *226*, 2015, p. 3651. doi:10.1007/s00707-015-1416-1
[25] Kang, J.-Y., Bacroix, B., Réglé, H., Oh, K. H., Lee, H.-C.: Acta Mater., *55*, 2007, p. 4935. doi:10.1016/j.actamat.2007.05.014
[26] Quey, R., Dawson, P. R., Driver, J. H.: J. Mech. Phys. Solids, *60*, 2012, p. 509. doi:10.1016/j.jmps.2011.11.005
[27] Sanchez, L. R., Hartfield-Wunsch, S.: SAE Int. J. Mater. Manuf., *4*, 2011, p. 826. doi:10.4271/2011-01-0535
[28] Hol, J., Meinders, V. T., Geijselaers, H. J. M., van den Boogaard, A. H.: Tribol. Int., *85*, 2015, p. 10. doi:10.1016/j.triboint.2014.12.017